



## Original Article

# Mangiferin induces cell death against rhabdomyosarcoma through sustained oxidative stress

Vishwanadha Vijaya Padma<sup>a,\*</sup>, Palanisamy Kalaiselvi<sup>a,1</sup>,  
Rangasamy Yuvaraj<sup>b</sup>, M. Rabeeth<sup>b</sup>

<sup>a</sup> Department of Biotechnology, Bharathiar University, Coimbatore, Tamil Nadu, India

<sup>b</sup> Department of Biotechnology, Kongunadu Arts and Science College, Coimbatore, Tamil Nadu, India

## ARTICLE INFO

## Article history:

Received 6 March 2014

Received in revised form

31 July 2014

Accepted 1 August 2014

Available online 2 October 2014

## Keywords:

antioxidants

cytotoxicity

mangiferin

oxidative stress

reactive oxygen species

## ABSTRACT

**Background:** Embryonic rhabdomyosarcoma (RD) is the most prevalent type of cancer among children. The present study aimed to investigate cell death induced by mangiferin in RD cells.

**Methods:** The Inhibitory concentration (IC<sub>50</sub>) value of mangiferin was determined by an MTT (3-(4,5-Dimethylthiazol-2-yl)-2,5-Diphenyltetrazolium Bromide) assay. Cell death induced by mangiferin against RD cells was determined through lactate dehydrogenase and nitric oxide release, intracellular calcium levels, reactive oxygen species generation, antioxidant status, mitochondrial calcium level, and mitochondrial membrane potential. Furthermore, acridine orange/ethidium bromide staining was performed to determine early/late apoptotic event.

**Results:** Mangiferin induced cell death in RD cells with an IC<sub>50</sub> value of 70 μM. The cytotoxic effect was reflected in a dose-dependent increase in lactate dehydrogenase leakage and nitric oxide release during mangiferin treatment. Mangiferin caused dose dependent increase in reactive oxygen species generation, intracellular calcium levels with subsequent decrease in antioxidant status (catalase, superoxide dismutase, glutathione-S-transferase, and glutathione) and loss of mitochondrial membrane potential in RD cells. Further data from fluorescence microscopy suggest that mangiferin caused cell shrinkage and nuclear condensation along with the occurrence of a late event of apoptosis.

**Conclusion:** Results of the present study shows that mangiferin can act as a promising chemopreventive agent against RD by inducing sustained oxidative stress.

© 2014 Korea Institute of Oriental Medicine. Published by Elsevier. This is an open access article under the CC-BY-NC-ND license (<http://creativecommons.org/licenses/by-nc-nd/4.0/>).

\* Corresponding author. Department of Biotechnology, Bharathiar University, Coimbatore 641 046, Tamil Nadu, India.

E-mail address: [Padma.vijaya@gmail.com](mailto:Padma.vijaya@gmail.com) (V.V. Padma).

<sup>1</sup> These authors contributed equally to this work.

<http://dx.doi.org/10.1016/j.imr.2014.09.006>

2213-4220/© 2014 Korea Institute of Oriental Medicine. Published by Elsevier. This is an open access article under the CC-BY-NC-ND license (<http://creativecommons.org/licenses/by-nc-nd/4.0/>).

## 1. Introduction

Cancer continues to represent the largest cause of mortality in the world.<sup>1</sup> Rhabdomyosarcoma (RD) is the most common type of cancer in children under the age of 15 years, and embryonal RD is its most common subtype that develops in the head and neck region and the genitourinary tract. Treatment of this cancer involves a combination of chemotherapy and radiation along with surgery. Chemotherapeutic agents currently available for treating RD have been found to possess several toxic effects such as hepatotoxicity and cardiotoxicity.<sup>2,3</sup> An extremely promising strategy employed for cancer prevention today involves the use of natural compounds. Several studies showed the protective or curative effect of phytochemicals against various diseases including cancer, and in-depth studies are being carried out to understand their mechanism of action. Among them, polyphenols, which are naturally present in plants, are of great interest as chemopreventive agents.<sup>4</sup>

Mangiferin (2-β-D-glucopyranosyl 1-1,3,6,7-tetrahydroxy xanthone), a xanthone C-glucoside from *Mangifera indica* L. (Anacardiaceae), is consumed worldwide as a fruit, and as a culinary and flavoring agent. Fruits, bark, and leaves of *M. indica* have been reported to possess diverse medicinal properties and are widely used in several medicinal preparations. Mangiferin has been reported to contain antioxidant, anti-tumor, antiviral, antibacterial, antihyperglycemic, analgesic, anti-inflammatory, antidiarrheal, anti-HIV, immunostimulant, and immunomodulatory properties.<sup>5-11</sup>

The antioxidant activity of mangiferin is attributed to its being a polyphenol.<sup>12</sup> Anticarcinogenic potential of mangiferin in bowel carcinogenesis<sup>9</sup> has been reported earlier. Mangiferin inhibited proliferation and induced apoptosis in K562 leukemia cells<sup>13</sup> and HL-60<sup>14</sup> in a dose- and time-dependent manner. Previous reports show that studies on the anticancer activities of polyphenols against RD are sparsely reported. Since mangiferin is a well-established pharmacophore, the present study was aimed at investigating the possible anticancer activity of mangiferin against RD cells.

## 2. Methods

### 2.1. Chemicals

Mangiferin, 2,7-dichlorodihydrofluorescein diacetate (DCF-DA), Fura 2-AM, Rhod 2-AM, and propidium iodide were purchased from Sigma Aldrich Chemicals Private Limited, Bangalore, India. Carbonyl cyanide 4-(trifluoromethoxy) phenylhydrazone (CCCP) and 3,3'-dihexyloxycarbocyanine iodide (DiOC<sub>6</sub>) were procured from Calbiochem, La Jolla, CA, USA. Dulbecco's modified eagles medium, fetal bovine serum, trypsin, antibiotics (penicillin, streptomycin, and gentamycin), and other fine chemicals were purchased from the Himedia Laboratories Private Limited, Mumbai, India.

### 2.2. Cell culture and solubility

RD cells were procured from the National Centre for Cell Science, Pune, India. The cells were maintained in DMEM + 10%

fetal bovine serum supplemented with antibiotics (100 units/mL penicillin, 30 μg/mL streptomycin, and 20 μg/mL gentamycin). The cells were grown in a CO<sub>2</sub> incubator (5% CO<sub>2</sub>, 37 °C). Cells at 80% confluency were trypsinized and used for assays. Mangiferin was dissolved in dimethyl sulfoxide; the final solvent concentration used in culture did not exceed 0.01%.

### 2.3. Cell viability

Cell viability was determined by an MTT assay.<sup>15</sup> Cells were seeded at a density of 10<sup>4</sup> cells/well and allowed to attach for 1 hour in a CO<sub>2</sub> incubator. Next, the cells were treated with mangiferin at various concentrations (10 μM, 30 μM, 50 μM, 70 μM, 90 μM, and 110 μM) for 24 hours. After the treatment schedule, MTT was added (5 mg/mL) and the cells were incubated for 5 hours. The formed purple formazon crystals were solubilized using dimethyl sulfoxide, and absorbance was measured at 570 nm in a spectrophotometer (Bio-Tek Instruments, Winooski, VT).

### 2.4. Treatment schedule

The treatment groups were as follows: Group I was the control group; Group II consisted of cells treated with mangiferin at a concentration of 50 μM, Group III consisted of cells treated with mangiferin at 70 μM, and Group IV consisted of cells treated with mangiferin at 90 μM. Cell count in each group was 5 × 10<sup>6</sup>. After attachment, the cells were treated with different concentrations of mangiferin (as mentioned in different treatment groups) and incubated for 24 hours.

After treatment, the supernatant was used for estimating the release of lactate dehydrogenase (LDH) and nitric oxide (NO). The cells were trypsinized and suspended in Tris-EDTA phenyl methyl sulfonyl fluoride buffer used for estimating the levels of DNA, RNA, protein, lipid peroxidation, and nonenzymic antioxidant [glutathione (GSH)], and activities of enzymic antioxidants such as super oxide dismutase, catalase, glutathione-S-transferase.

### 2.5. Cytostatic effect

Cytostatic effect of mangiferin on RD cells was determined by estimating the levels of DNA, RNA, and protein. The cell suspension was treated with 5% Trichloro acetic acid (TCA) to precipitate nucleic acids and proteins. The precipitate was washed with 10% TCA (ice cold) and 95% ethanol to remove lipids. To the resulting precipitate 5% TCA was added and the mixture was incubated at 70 °C for 15 minutes. After centrifugation (10,000 g for 10 minutes), the supernatant was used for DNA and RNA estimation.

### 2.6. Estimation of DNA

To the nucleic acid extract, 1N perchloric acid and diphenylamine reagent were added and the mixture was incubated at 95 °C for 10 minutes. A blank and the standard (calf thymus DNA) samples were also tested concurrently. Absorbance was read at 640 nm, and the values were expressed as μg/5 × 10<sup>6</sup> cells.<sup>16</sup>

### 2.7. Estimation of RNA

To the nucleic acid extract, 5% TCA was added to make up the volume to 2.0 mL. To this, 3.0 mL of orcinol ferric chloride reagent was added and the mixture was incubated at 95 °C for 20 minutes. Absorbance was read at 640 nm, and values were expressed as  $\mu\text{g}/5 \times 10^6$  cells Rawal et al.<sup>17</sup>

### 2.8. Estimation of protein

Protein was estimated following the procedure described by Lowry et al.<sup>18</sup>

### 2.9. Release of LDH

The supernatant from the different treatment groups was used for the assay of LDH, as described by Nieland.<sup>19</sup> The principle involves conversion of lithium lactate to pyruvate, and the color developed in the presence of Nicotinamide Adenine Dinucleotide (NAD) and dinitrophenyl hydrazine was measured at 420 nm. The results were expressed as % LDH release compared to the control group.

### 2.10. Nitric oxide assay

The nitrite concentration in the supernatant was measured using Griess reagent at 540 nm.<sup>20</sup>

### 2.11. Estimation of protein, and nonenzymic and enzymic antioxidant status

Cell extracts were prepared by sonication using a buffer (50 mM Tris, 5 mM EDTA, 10  $\mu\text{g}/\text{mL}$  phenyl methyl sulfonyl fluoride, pH 7.6). After sonication, the extract was centrifuged (4000  $\times$  2500 g, 5 minutes, 4 °C), and the supernatant was isolated and used for the assays. Protein concentration was determined by Lowry et al.<sup>18</sup>

### 2.12. Total reduced GSH

Estimation of the total reduced GSH was carried out following the procedure described by Moron et al.<sup>21</sup> After precipitation of protein using TCA, the supernatant was treated with DTNB (5,5'-dithiobis-(2-nitrobenzoic acid)) and absorbance was measured at 412 nm. The GSH content was determined using the standard GSH concentration and expressed as nmoles of GSH/mg of protein.

### 2.13. Antioxidant enzyme activities (glutathione-S-transferase, catalase, and superoxide dismutase)

Glutathione-S-transferase activity was determined according to Habig et al.<sup>22</sup> The reaction mixture contained 50  $\mu\text{g}$  protein in 0.1 M phosphate buffer (pH 6.5), 1 mM 1-chloro-2,4-dinitrobenzene (CDNB), and 1 mM GSH in a final volume of 3 mL. The change in absorbance (340 nm) was measured at every 30 seconds for 3 minutes in a UV-visible double-beam spectrophotometer. The enzyme activity was expressed as nmoles of CDNB conjugated/min/mg protein. Catalase

activity was determined following the method described by Aebi.<sup>23</sup> The reaction mixture contained 50  $\mu\text{g}$  of protein in phosphate buffer (50 mM, pH 7.0).  $\text{H}_2\text{O}_2$  (10 mM) was added to initiate the reaction. Change in absorbance (240 nm) was measured every 30 seconds for 3 minutes. The enzyme activity was expressed as  $\mu\text{moles}$  of  $\text{H}_2\text{O}_2$  utilized/min/mg protein. Superoxide dismutase activity was measured as described by Marklund and Marklund.<sup>24</sup> The assay mixture contained 50  $\mu\text{g}$  of protein in 50 mM Tris-cacodylic acid buffer (pH 8.2), and pyrogallol solution (0.2 mM) and EDTA (1 mM). Auto-oxidation of pyrogallol was measured at 420 nm every 30 seconds for 3 minutes (1 unit = the amount of enzyme required to inhibit pyrogallol auto-oxidation by 50%).

### 2.14. Estimation of lipid peroxidation

Lipid peroxidation was determined according to Okhawa et al.<sup>25</sup> To the cell extract were added 8% Sodium dodecyl sulfate (SDS) and 0.8% Thiobarbituric acid (TBA) in 20% acetic acid. The final reaction volume was made up with distilled water and the mixture was heated at 90 °C for 60 minutes in a water bath. The tubes were allowed to cool; butanol/pyridine mixture was added to these and shaken vigorously. An organic layer was isolated after centrifugation at 4000 rpm for 10 minutes and measured at 532 nm. The lipid peroxide content was expressed as nmoles of TBA reactants/mg of protein.

### 2.15. Measurement of intracellular reactive oxygen species generation

Cells at a density of  $1 \times 10^5$  cells/well were incubated with 25  $\mu\text{L}$  of DCF-DA for 30 minutes. After 30 minutes, the cells were incubated with different concentrations of mangiferin for different time periods. The samples were centrifuged at 1500 rpm for 10 minutes. To the cell pellet, 1.0 mL of phosphate buffered saline (PBS) was added and fluorescence emission was measured at the excitation (480 nm) and emission (520 nm) wavelengths using a Hitachi spectrofluorimeter (Hitachi Co., Tokyo, Japan).<sup>26</sup> The whole experiment was performed in dark condition. The values were compared with those of the control group and expressed as % DCF fluorescence.

### 2.16. Measurement of intracellular calcium levels

Intracellular calcium ( $[\text{Ca}^{2+}]_i$ ) was analyzed as described by Sul et al.<sup>27</sup> The cells at a density of  $1 \times 10^6$  cells/well were treated with different concentrations of mangiferin and incubated for 24 hours. After the treatment schedule, 5  $\mu\text{M}$  Fura 2-AM in calcium buffer was added and the mixture was further incubated for 1 hour. Cells were washed with PBS, trypsinized, and suspended in 1.0 mL PBS. Fluorescence emission was monitored at the excitation wavelength of 510 nm and emission wavelength cycling between 340 nm and 380 nm using a fluorimeter. The  $[\text{Ca}^{2+}]_i$  level is proportional to the ratio of intensities at 340 nm and 380 nm. The values are expressed as % Fura 2-AM fluorescence when compared with the control group.

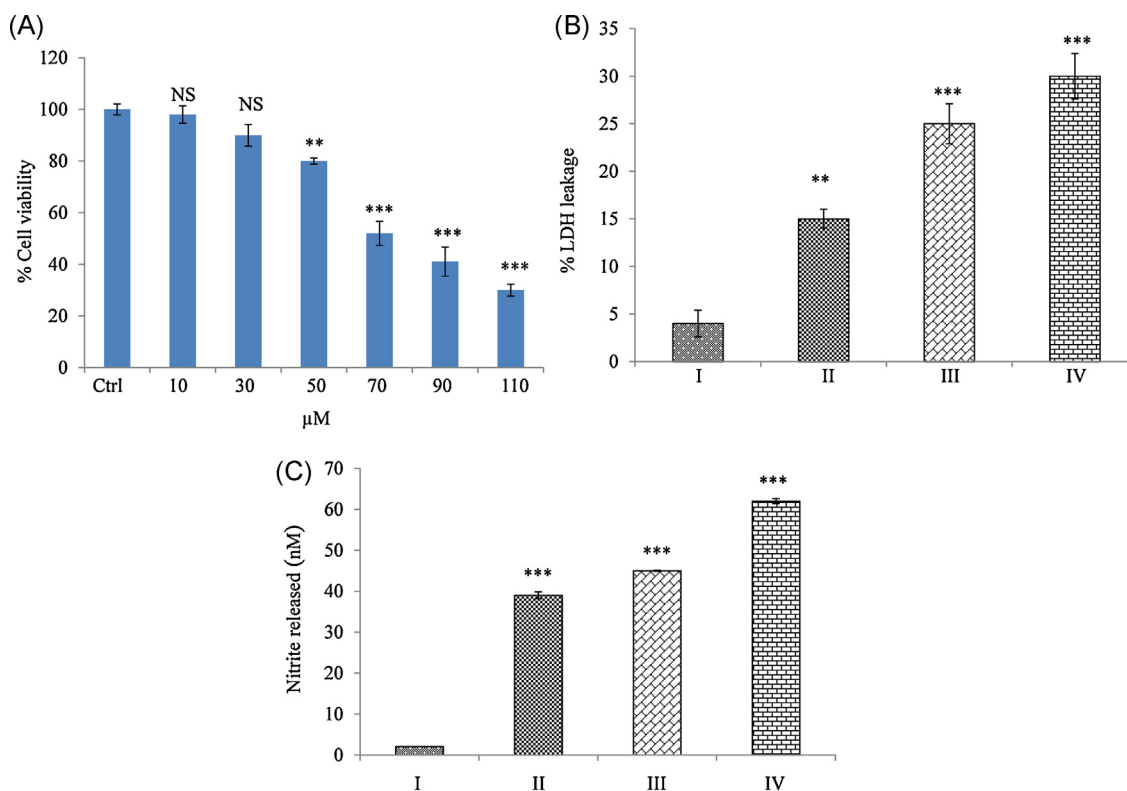


**Fig. 1 – Cytotoxic effect of mangiferin on rhabdomyosarcoma cells. (A) Cell viability by MTT assay: Cell viability was expressed in percentage while compared with the control group ( $IC_{50} = 70 \mu\text{M}$ ). (B) LDH leakage: Mangiferin caused a dose-dependent increase in LDH release. Results were expressed as % LDH leakage when compared with the control group. (C) Nitrite release: A dose-dependent increase in nitrite release was observed when compared with the control group. Results were expressed as nmoles of nitrite released. Results shown are mean  $\pm$  SD ( $n = 6$ ).**

Significant differences were indicated as follows:

\*  $p < 0.01$ .

\*\*\*  $p < 0.001$ .

Group I, control group; Group II, 50  $\mu\text{M}$  mangiferin group; Group III, 70  $\mu\text{M}$  mangiferin group; Group IV, 90  $\mu\text{M}$  mangiferin group; LDH, lactate dehydrogenase; NS, nonsignificant; SD, standard deviation.

### 2.17. Measurement of mitochondrial calcium levels

Mitochondrial  $\text{Ca}^{2+}$  ( $[\text{Ca}^{2+}]_m$ ) levels were analyzed using the Rhod 2-AM (mitochondrial  $\text{Ca}^{2+}$ -sensitive fluorescent dye) cold/warm incubation protocol.<sup>28</sup> Cells ( $1 \times 10^6$  cells/well) were treated with different concentrations of mangiferin and incubated for 24 hours. After 24 hours, the cells were washed in PBS and loaded with Rhod 2-AM (1  $\mu\text{M}$ ) for 120 minutes at 4 °C, followed by incubation at 37 °C for 30 minutes. After incubation, the cells were washed with PBS, trypsinized, and suspended in 1.0 mL PBS. Mitochondrial calcium levels were detected with a fluorescence spectrophotometer (excitation/emission: 533/576 nm). The values are calculated as % relative Rhod-fluorescence as compared to the control group.

### 2.18. Measurement of mitochondrial membrane potential ( $\Delta\psi_M$ )

The cells ( $1 \times 10^6$  cells/well) were treated with different concentrations of mangiferin and incubated for 24 hours. After

24 hours, the cells were washed with PBS and incubated with 50 nM DiOC<sub>6</sub><sup>3</sup> at 37 °C for 30 minutes. Simultaneously a positive control of CCCP (50  $\mu\text{M}$ ; carbonyl cyanide m-chlorophenyl hydrazone) was maintained. CCCP was added to the positive control group 15 minutes prior to the addition of DiOC<sub>6</sub><sup>3</sup>. DiOC<sub>6</sub><sup>3</sup> was removed and the cells were suspended in 1.0 mL PBS.<sup>3</sup> The readings were taken at an excitation wavelength of 488 nm and an emission wavelength of 500 nm in a fluorimeter.<sup>29</sup> The values are expressed as % relative fluorescence as compared to the control group.

### 2.19. Analysis of early/late apoptotic event: Acridine orange/ethidium bromide staining

The cells ( $1 \times 10^6$  cells/well) were treated with different concentrations of mangiferin and incubated for 24 hours at 37 °C. Next, the cells were washed with PBS, and acridine orange/ethidium bromide (AO/ETBR) was added (1  $\mu\text{g}/\text{mL}$  each). After 30 minutes, the cells were pelleted down, suspended in PBS and mounted on a slide. Images were captured by an Olympus fluorescent microscope using a green filter

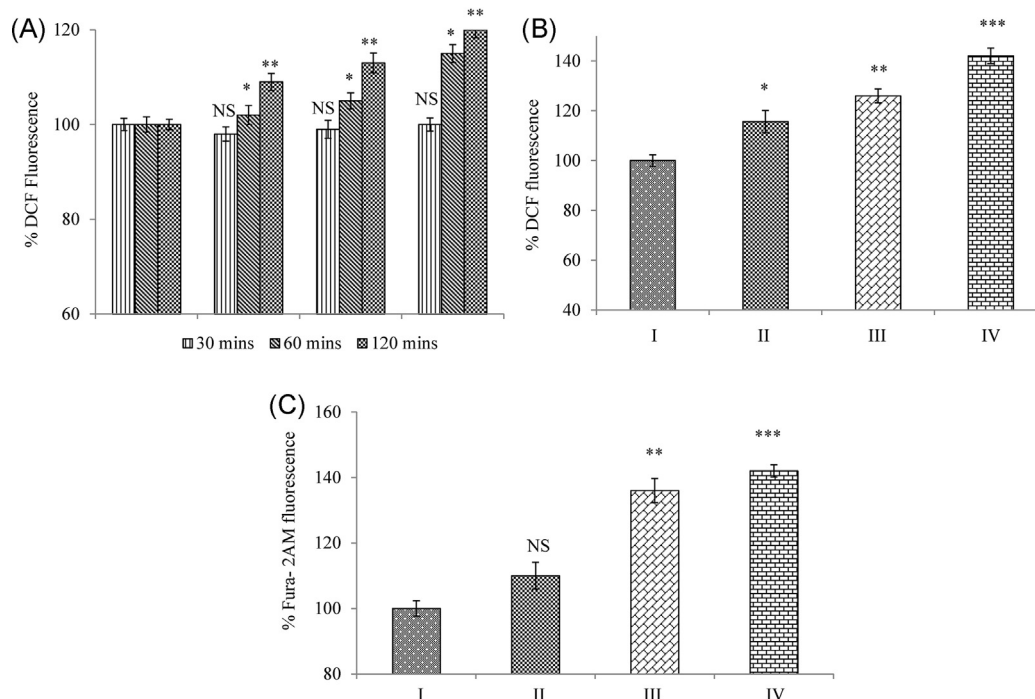


**Fig. 2 – Mangiferin induces ROS generation and  $[Ca^{2+}]_i$  levels in RD cells. (A) Time course—ROS generation: Mangiferin caused an early rise in ROS generation (1 hour) when compared with the control cells. (B) Dose-dependent ROS generation: A dose-dependent increase in ROS accumulation was observed at 24 hours. Results were expressed as % ROS generation. (C)  $[Ca^{2+}]_i$  levels: A dose-dependent increase in intracellular calcium was observed during mangiferin treatment. Results were expressed as % relative Fura 2-AM fluorescence. Results shown are mean  $\pm$  SD ( $n = 6$ ).**

Significant differences were indicated as follows:

\*  $p < 0.05$ .

\*\*  $p < 0.01$ .

\*\*\*  $p < 0.001$ .

$[Ca^{2+}]_i$ , intracellular calcium levels; DCF, 2,7-dichlorodihydrofluorescein; Group I, control group; Group II, 50  $\mu$ M mangiferin group; Group III, 70  $\mu$ M mangiferin group; Group IV, 90  $\mu$ M mangiferin group; NS, nonsignificant; RD, rhabdomyosarcoma; ROS, reactive oxygen species; SD, standard deviation.

(excitation wavelength 536 nm and emission wavelength 617 nm).<sup>30</sup>

## 2.20. Statistical analysis

Data were analyzed using Student *t* test. Differences in *p* values (\*  $p < 0.05$ , \*\*  $p < 0.01$ , and \*\*\*  $p < 0.001$ ) were considered as statistically significant. Data are expressed as mean  $\pm$  standard deviation.

## 3. Results

### 3.1. Mangiferin induces cytotoxicity by LDH and NO release

To assess the cytotoxicity, cells were treated with mangiferin for 24 hours, and the cell viability was determined using an MTT assay. Mangiferin caused cell death dose dependently.  $IC_{50}$  value was found to be 70  $\mu$ M, which is significantly ( $p < 0.001$ ) different from that of the control group (Fig. 1A). Further experiments were carried out with control-untreated cells (Group I), 50  $\mu$ M mangiferin (Group II), 70  $\mu$ M Mangiferin

(Group III), and 90  $\mu$ M mangiferin (Group IV). Loss of cell membrane integrity induces the release of membrane-bound LDH into the cell culture medium, which is directly related to cytotoxicity. Nitrite is the stable end product of NO. NO can regulate many physiological processes *in vivo* and *in vitro* through S-nitrosothiols, which cause damage to DNA, protein, and lipid molecules, ultimately leading to apoptosis.<sup>31</sup> Fig. 1B, 1C shows a dose-dependent increase in LDH and NO concentrations when compared with the control group.

### 3.2. Mangiferin caused $[Ca^{2+}]_i$ release and accumulation of reactive oxygen species in RD cells

Oxidative stress and changes in  $[Ca^{2+}]_i$  can induce mitochondrial pore opening through oxidization of membrane protein thiol groups. We therefore used DCF-DA and Fura 2-AM fluorescent dye to measure the concentration of reactive oxygen species (ROS) generated and  $[Ca^{2+}]_i$  levels, respectively, by the spectrofluorimetric method. The rise in ROS level was evident as early as 1 hour of addition of the dye, and increased accumulation of ROS was observed at 24 hours in a dose-dependent manner when compared with the control group (Fig. 2A, 2B).



A dose-dependent increase in the levels of  $[Ca^{2+}]_i$  levels was observed when compared with the control group (Fig. 2C).

### 3.3. Mangiferin enhanced $[Ca^{2+}]_m$ and disrupted mitochondrial membrane potential ( $\Delta\psi_m$ ) in RD cells

We next determined whether mangiferin causes an increase in mitochondrial  $Ca^{2+}$  concentrations using Rhod 2-AM. Fig. 3A shows a dose-dependent increase in  $[Ca^{2+}]_m$  when compared with the control group. DiOC<sub>6</sub> is a carbocyanine derivative with short alkyl tails.<sup>3</sup> It decreases fluorescence by accumulation on hyperpolarized membranes.<sup>3</sup> Fig. 3B shows a dose-dependent loss of mitochondrial membrane potential when compared with the control group.

### 3.4. Mangiferin causes an imbalance in lipid peroxidation and antioxidant status

Increased generation and accumulation of ROS damages membrane phospholipids and also causes an imbalance in the antioxidant status of the cells. Damage to the phospholipids initiates lipid peroxidation. Mangiferin caused a significant increase in Thiobarbituric acid reactive substances (TBARS) levels in a dose-dependent manner. GSH is the major intracellular nonprotein thiol, and its redox status is critical for various biological events.<sup>32</sup> In mangiferin-treated cells, there was a significant reduction in the levels of GSH in a dose-dependent manner (Table 1). Antioxidant enzymes prevent oxidative stress by their defense mechanisms. The present study showed that mangiferin treatment significantly decreased the antioxidant status in a dose-dependent manner (Table 1).

**Table 1 – Mangiferin dose dependently affects levels of biomolecules in RD cells\***

Group	DNA	RNA	Protein
I	5.3 ± 0.7	7.4 ± 1.4	92.5 ± 5.1
II	4.1 ± 0.4***	6.7 ± 1.2**	72.5 ± 4.8***
III	3.2 ± 0.6***	5.5 ± 1.1***	58.5 ± 4.4
IV	2.1 ± 0.5	3.9 ± 0.5	42.3 ± 4.2

Values are expressed as  $\mu\text{g}/5 \times 10^6$  cells. Results shown are mean  $\pm$  SD ( $n=6$ ). Statistical analysis of the data was performed using the Student t test.

\* Statistical significance was obtained when groups treated with different concentrations of mangiferin were compared with the control group.

\*\*  $p < 0.05$ .

\*\*\*  $p < 0.01$ .

$p < 0.001$ .

Group I, control group; Group II, 50  $\mu\text{M}$  mangiferin group; Group III, 70  $\mu\text{M}$  mangiferin group; Group IV, 90  $\mu\text{M}$  mangiferin group; RD, rhabdomyosarcoma; SD, standard deviation.

### 3.5. Effect of mangiferin on the levels of biomolecules (DNA, RNA, and protein)

In the presence of ROS, phenolic compounds undergo redox cycling and form phenoxyl radicals. These compounds cause damage to various biological molecules inside the cell.<sup>33</sup> Table 2 shows a significant decrease in the levels of biomolecules (DNA, RNA, and protein) in mangiferin-treated cells.

### 3.6. Mangiferin induces apoptosis in RD cells

AO/ETBR double staining was performed to identify the cell death induced by mangiferin (early or late apoptotic/necrosis;

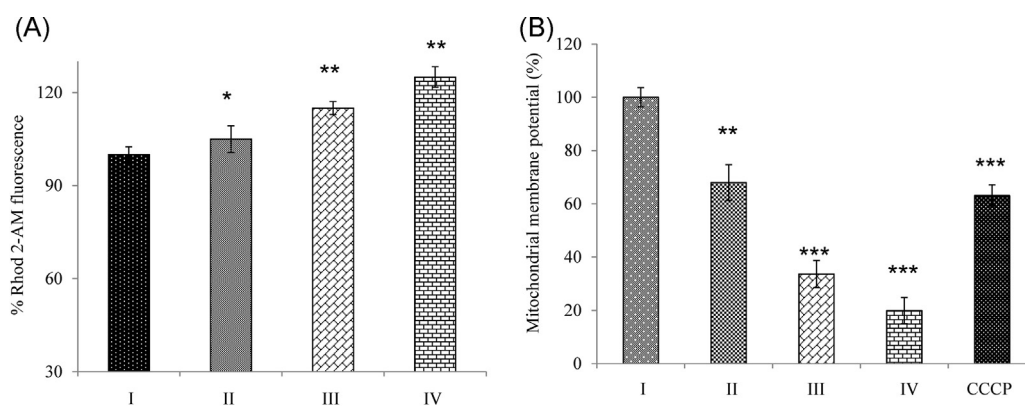


**Fig. 3 – Mangiferin modulates  $[Ca^{2+}]_m$  and induces loss of mitochondrial membrane potential. (A)  $[Ca^{2+}]_m$  levels: Mangiferin caused significant changes in  $[Ca^{2+}]_m$  in a dose-dependent manner. Results were expressed as % relative Rhod 2-AM fluorescence. (B) Mitochondrial membrane potential ( $\Delta\psi_m$ ): A dose-dependent significant loss of membrane potential was observed during mangiferin treatment. The cells were treated with 50  $\mu\text{M}$  CCCP as a positive control. Results shown are mean  $\pm$  SD ( $n=6$ ).**

Significant differences were indicated as follows:

\*  $p < 0.05$ .

\*\*  $p < 0.01$ .

\*\*\*  $p < 0.001$ .

$[Ca^{2+}]_m$ , mitochondrial calcium levels; CCCP, carbonyl cyanide 4-(trifluoromethoxy) phenylhydrazone; Group I, control group; Group II, 50  $\mu\text{M}$  mangiferin group; Group III, 70  $\mu\text{M}$  mangiferin group; Group IV, 90  $\mu\text{M}$  mangiferin group; NS, nonsignificant; SD, standard deviation.

**Table 2 – Effect of mangiferin on antioxidant status and lipid peroxidation levels**

Group <sup>¶</sup>	GSH <sup>a</sup>	SOD <sup>†</sup>	CAT <sup>‡</sup>	GST	LPO <sup>  </sup>
I	32.5 ± 2.7	30.6 ± 1.9	23.4 ± 1.5	25.6 ± 2.5	5 ± 0.51
II	29.5 ± 2.1**	26.4 ± 1.7**	21.4 ± 1.2*	21.6 ± 2.2**	14 ± 0.63*
III	24.5 ± 1.7***	20.6 ± 1.9***	15.4 ± 1.1**	17.6 ± 2.1**	22 ± 0.47**
IV	21.5 ± 1.9***	17.6 ± 1.8***	11.4 ± 1.5***	14.3 ± 1.8***	27 ± 0.12**

<sup>a</sup> GSH content was expressed as nM of GSH/mg of protein.

<sup>†</sup> SOD 1 U is the amount of enzyme required for 50% inhibition of pyrogallol auto-oxidation.

<sup>‡</sup> Catalase 1 U is the enzyme that consumes 1 nmole H<sub>2</sub>O<sub>2</sub>/minute.

GST 1 U represents the enzyme that conjugates 1 μmole CDNB/min.

<sup>||</sup> LPO was expressed as TBA reactants (nM)/mg of protein.

<sup>¶</sup> Statistical significance was obtained when different concentrations of mangiferin-treated groups were compared with the control group.

\*  $p < 0.05$ .

\*\*  $p < 0.01$ .

\*\*\*  $p < 0.001$ .

CAT, catalase; Group I, control group; Group II, 50 μM mangiferin group; Group III, 70 μM mangiferin group; Group IV, 90 μM mangiferin group; GSH, glutathione; GST, glutathione-S-transferase; LPO, lipid peroxidation; SOD, superoxide dismutase.

Fig. 4). Control cells (Fig. 4A) were stained uniformly, which appeared as green nuclei with intact nuclear membranes. Cells treated with 50 μM mangiferin showed nuclear condensation (Fig. 4B). Cells treated with 70 μM (Fig. 4C) and 90 μM (Fig. 4D) mangiferin showed late apoptosis, while the nuclei appeared orange with chromatin condensation and intranucleosomal formation. Fig. 5 shows the percentage of viable and apoptotic cells during mangiferin treatment.

#### 4. Discussion

RD is the most invasive tumor that targets the head and neck regions.<sup>34</sup> Attempts to alleviate this cancer have led to the development of certain drugs, but these drugs are found to cause various toxic effects. Chemotherapy is the only way to efficiently treat these cancers without any side effects. In recent years, it has been documented that polyphenols and flavanoids possess antioxidant or pro-oxidant activities, depending on the environment in which they are present as well as the concentration used. These compounds are excellent targets for chemoprevention because they act as pro-oxidants in an environment with an excessive amount of ROS, as in cancer cells. Mangiferin isolated from the bark of *M. indica* can act as a pro-oxidant at a high concentration, which can efficiently target cancer cells.<sup>35</sup> The present study showed that mangiferin induced cell death in RD cells with an IC<sub>50</sub> value of 70 μM. LDH is a cytosolic enzyme, and membrane damage due to cytotoxicity leads to an increase in the release of this enzyme from the cell. The increase in the LDH during mangiferin treatment implies that mangiferin causes severe damage to cells, leading to cytotoxicity.

NO plays a major role in cellular signaling; however, at higher concentrations it exhibits cytotoxic effects. NO causes nitration and nitrosylation of proteins and damages DNA.<sup>36</sup> In addition, one of the most sensitive targets of NO is GSH. Reports suggest that NO induces GSH depletion, thereby sensitizing the cells for NO-mediated cytotoxicity.<sup>37</sup> Increased levels of GSH caused resistance of RD to vincristine, which was overcome by buthionine sulfoximine-mediated GSH depletion.<sup>38</sup> A significant increase in NO levels with

concomitant depletion in levels of GSH might be attributed to cell death induced by mangiferin in RD cells.

The mangiferin-induced early rise in ROS levels was found to increase in a sustained manner, suggesting it to be an important mediator in mangiferin-induced cell death. Earlier reports suggest that under the conditions of enhanced mitochondrial ROS generation, mangiferin gives rise to the oxidized products of semiquinone radicals and quinines, which further potentiate the oxidative stress.<sup>35</sup> The generated ROS attack various biomolecules in the cells, of which polyunsaturated fatty acids in the membrane are sensitive and prone to oxidation. These ROS act on the methylene group present between the double bonds of the Polyunsaturated fatty acids (PUFA) and initiate lipid peroxidation.<sup>39</sup> These fatty acid oxidation products exacerbate stress conditions inside the cells. Normally, the cells are equipped with the antioxidant defense mechanism to efficiently remove these toxic substances generated by free radical attack. The antioxidant enzymes superoxide dismutase, catalase, and GSH are involved in the cellular defense and protect cells against free radical damage. It has been documented that, in its defense mechanism to prevent the oxidative stress, GSH forms adducts with oxidation products of mangiferin, leading to further generation of ROS.<sup>35,40</sup> Similar reactions have been reported in quercetin, involving the formation of quercetin glutathionyl adducts.<sup>41</sup> Quercetin glutathionyl adduct-induced damages to DNA and protein have been documented in case of cancer cells.<sup>42</sup> An imbalance in redox homeostasis enhances the accumulation of free radicals.<sup>43</sup> Thus, the observed reduction in the antioxidant status might be explained as the inability of the cells to counteract the overwhelmed oxidative stress situation created by mangiferin.

Ca<sup>2+</sup> levels regulate various cellular signaling, so maintenance of calcium levels is a prerequisite for normal cellular processes. Because mitochondria have the highest Ca<sup>2+</sup> accumulation capacity, increased levels of [Ca<sup>2+</sup>]<sub>i</sub> levels modulate mitochondrial calcium homeostasis.<sup>44</sup> In addition, increases in Ca<sup>2+</sup> levels are sensitive to various events occurring in mitochondria, such as ATP production, ROS generation, and mitochondrial membrane potential, which in turn lead to the release of proapoptotic proteins.<sup>45</sup> Increases in ROS and [Ca<sup>2+</sup>]<sub>i</sub> levels are implicated in oxidizing the thiol interactions

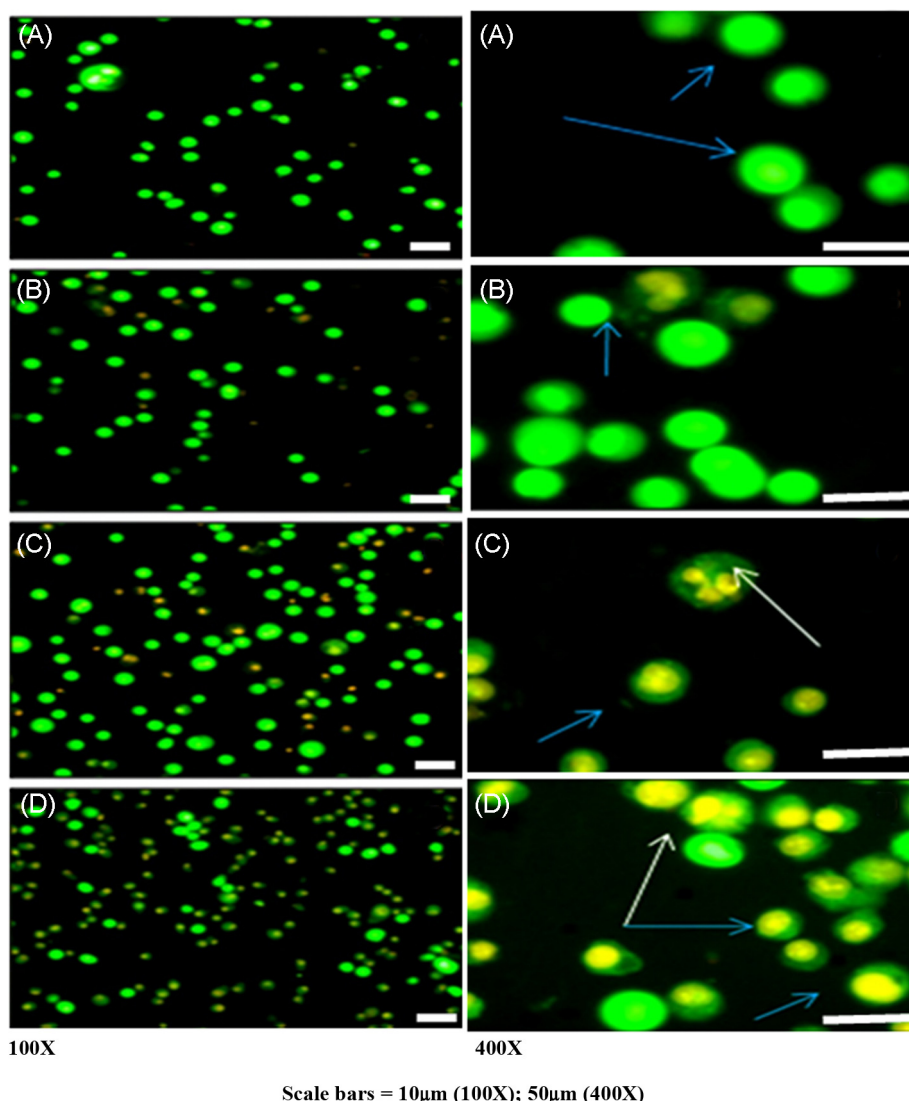


**Fig. 4 – Mangiferin induces late apoptotic event in rhabdomyosarcoma cells. Early/late apoptotic event or necrosis induced by mangiferin in RD cells was analyzed by acridine orange/ETBR staining [magnification 100× and 400×; scale bar: 100× (10 μm); 400× (50 μm)]. (A) Control cells show bright green nuclei with intact plasma and nuclear membrane. (B) Cells treated with 50 μM mangiferin show minimal cell damage with nuclear condensation. (C) Cells treated with 70 μM mangiferin show cells with late apoptosis with intranucleosomal DNA (white arrows). (D) Cells treated with 90 μM mangiferin show late apoptotic event, with nuclei appearing in orange with condensed chromatin (blue arrows) and intranucleosomal DNA (white arrows).**

**ETBR, ethidium bromide; RD, rhabdomyosarcoma.**

in mitochondrial membrane, leading to the loss of mitochondrial membrane potential. One of the early events in apoptosis includes dissipation of mitochondrial membrane potential. In the present study, the loss of mitochondrial membrane potential was associated with an increase in  $[Ca^{2+}]_i$  and ROS generation. The present findings of mangiferin-induced oxidative stress corroborate with earlier observations of Pardo-Andreu et al.<sup>35</sup>

Loss of mitochondrial membrane potential subsequently releases apoptotic proteins and executes cell death.<sup>46</sup> Morphological changes during apoptosis can be studied well using fluorescent staining techniques. Depending on the fluorescent properties of fluorochromes, it is possible to characterize

the mode of cell death (early or late apoptosis/necrosis). Fluorochromes such as AO and ETBR have specificity for nucleic acids; however, AO can enter into viable and apoptotic cells, while ETBR can enter only into the cells with late apoptosis and necrosis. Viable cells stained with AO emit a green fluorescence and have an intact nucleus, while early apoptotic cells appear to have a green nucleus with chromatin condensation and nuclear membrane blebbing. In cells exhibiting late apoptosis stain with both AO and ETBR, the nuclei appear orange with chromatin condensation. Necrotic cells are stained only by ETBR, and thus appear orange with an intact structure. Differential scoring with AO/ETBR showed a late event of apoptosis during mangiferin treatment. Mangiferin-induced



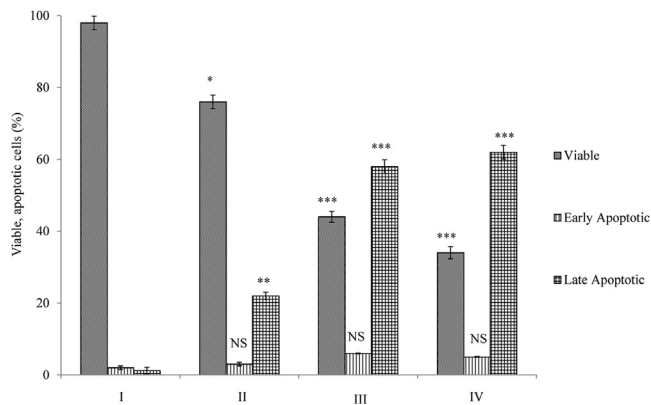


**Fig. 5 – Percentage of viable and apoptotic cells. Cells treated with mangiferin were analyzed for cell death using AO/ETBR staining. A total of 200 cells per treatment group were screened and analyzed for the differential uptake of AO/ETBR. Significant increase in induction of late apoptosis was observed at 50  $\mu$ M (\*  $p < 0.05$ ), 70  $\mu$ M ( $\dagger p < 0.001$ ), and 90  $\mu$ M ( $\ddagger p < 0.001$ ).**

**AO, acridine orange; ETBR, ethidium bromide; NS, nonsignificant levels of early apoptosis.**

anticancer effects have been reported in various other cell lines.<sup>47-49</sup>

In conclusion, the study shows that mangiferin induced cytotoxicity and apoptosis in RD cells through sustained oxidative stress and depletion of antioxidant status. The results suggest a potential anticancer effect of mangiferin against RD. Further research is required to study the molecular mechanism through which mangiferin exerts its effect on RD.

## Conflicts of interest

The authors declare no conflicts of interest.

## REFERENCES

- Abdullaev FI, Rivera LR, Roitenburd B, Espinosa AJ. Pattern of childhood cancer mortality in Mexico. *Arch Med Res* 2000;31:526-31.
- Torti FM, Bristow MM, Lum BL, Carter SK, Howes AE, Aston DA, et al. Cardiotoxicity of epirubicin and doxorubicin: assessment by endomyocardial biopsy. *Cancer Res* 1986;46:3722-7.
- Paschke R, Heine M, Braun S, Usadel KH. Mechanisms of hepatotoxicity caused by dacarbazine in rats. *J Cancer Res Clin Oncol* 1993;119:475-81.
- Sun J, Chu YF, Wu X, Liu RH. Antioxidant and antiproliferative activities of common fruits. *J Agric Food Chem* 2002;50:7449-54.
- Guha S, Ghosal S, Chattopadhyay U. Antitumor, immunomodulatory and anti-HIV effect of mangiferin, a naturally occurring glucosylxanthone. *Chemotherapy* 1996;42:443-51.
- Sanchez GM, Re L, Giuliani A, Nunez-Selles AJ, Davison GP, Leon-Fernandez OS. Protective effects of *Mangifera indica* L.

extract, mangiferin and selected antioxidants against TPA-induced biomolecules oxidation and peritoneal macrophage activation in mice. *Pharmacol Res* 2000;42:565-73.

- Scartezzini P, Speroni E. Review on some plants of Indian traditional medicine with antioxidant activity. *J Ethnopharmacol* 2000;71:23-43.
- Miura T, Ichiki H, Hashimoto I, Iwamoto N, Kato M, Kubo M, et al. Antidiabetic activity of a xanthone compound, mangiferin. *Phytomedicine* 2001;8:85-7.
- Yoshimi N, Matsunaga K, Katayama M, Yamada Y, Kuno T, Qiao Z, et al. The inhibitory effects of mangiferin, a naturally occurring glucosylxanthone, in bowel carcinogenesis of male F344 rats. *Cancer Lett* 2001;163:163-70.
- Garcia D, Leiro J, Delgado R, Sanmartin ML, Ubeira FM. *Mangifera indica* L. extract (Vimang®) and mangiferin modulate mouse humoral immune response. *Photother Res* 2003;17:1182-7.
- Leiro J, Arranz JA, Yanez M, Ubeira FM, Sanmartin ML, Orallo F. Expression profiles of genes involved in the mouse nuclear factor- $\kappa$ B signal transduction pathway are modulated by mangiferin. *Int Immunopharmacol* 2004;4:763-78.
- Martinez G, Delgado R, Perez G, Garrido G, Nunez-Selles A, Leon O. Evaluation of the *in vitro* antioxidant activity of *Mangifera indica* L. extracts (Vimang). *Photother Res* 2000;14:424-7.
- Cheng P, Peng ZG, Yang J, Song SJ. The effect of mangiferin on telomerase activity and apoptosis in leukemic K562 cells. *Zhong Yao Cai* 2007;30:306-9.
- Percival SS, Talcott ST, Chin ST, Mallak AC, Lounds-Singleton A, Pettit-Moore J. Neoplastic transformation of BALB/3T3 cells and cell cycle of HL-60 cells are inhibited by mango (*Mangifera indica* L.) juice and mango juice extracts. *J Nutr* 2006;136:1300-4.
- Mossman T. Rapid colorimetric assay for cellular growth and survival: application to proliferation and cytotoxicity assays. *J Immunol Methods* 1983;65:55-63.
- Burton KC. A study on the condition and mechanism of the diphenylamine reaction for the colorimetric estimation of deoxyribonucleic acid. *Biochem J* 1956;62:315-23.
- Rawal VM, Patel US, Rao GN, Desai RR. Clinical and biochemical studies on cataractous human lenses I—quantitative study of protein, RNA and DNA. *Arogyaa J Health Sci* 1977;3:69-72.
- Lowry OH, Rosenbrough NJ, Farr AL, Randall RJ. Protein measurement with Folin-phenol reagent. *J Biol Chem* 1951;193:265-75.
- Nieland AA. Lactic acid dehydrogenase of heart muscle. In: *Methods in enzymology*. New York: Academic Press; 1955, p. 394.
- Stuehr DJ, Marletta MA. Induction of nitrite and nitrate synthesis in murine macrophage by BCG infection, lymphokines, or interferon-gamma. *J Immunol* 1987;139:518-20.
- Moron MS, Depierre JW, Mannervik B. Levels of glutathione, glutathione reductase and glutathione S-transferase activities in rat lung and liver. *Biochem Biophys Acta* 1979;582:67-78.
- Habig WH, Smith TW, Leaf A. Glutathione-S-transferase: the first enzymatic step in mercapturic acid formation. *J Biol Chem* 1974;249:7130-9.
- Aebi H. Catalase. In: Bergmeyer HU, editor. *Methods of enzymatic analysis*. New York, NY, USA: Verlag Chemic Academic Press Inc; 1974:673-85.
- Marklund SL, Marklund GE. Involvement of the superoxide anion radical in the autoxidation of pyrogallol and a convenient assay for superoxide dismutase. *Eur J Biochem* 1974;47:469-74.

25. Okhawa H, Olishi N, Yasi K. Assay for lipid peroxides in animal tissues by thiobarbituric acid reaction. *Anal Biochem* 1979;95:351–8.
26. Jia SJ, Jiang DJ, Hu CP, Zhang XH, Deng HW, Li YJ. Lysophosphatidylcholine-induced elevation of asymmetric dimethylarginine level by the NADPH oxidase pathway in endothelial cells. *Vascul Pharmacol* 2006;44:143–8.
27. Sul D, Kim HS, Cho EK, Lee M, Kim HS, Jung WW, et al. 2,3,7,8-TCDD neurotoxicity in neuroblastoma cells is caused by increased oxidative stress, intracellular calcium levels, and tau phosphorylation. *Toxicology* 2009;255:65–71.
28. Trollinger DA, Cascio WE, Lemasters JJ. Mitochondrial calcium transients in adult rabbit cardiac myocytes: inhibition by ruthenium red and artifacts caused by lysosomal loading of Ca<sup>2+</sup>—indicating fluorophores. *Biophys J* 2000;79:39–50.
29. Marchetti P, Hirsch T, Zamzami N, Castedo M, Decaudin D, Susin SA, et al. Mitochondrial permeability transition triggers lymphocyte apoptosis. *J Immunol* 1996;157:4830–6.
30. Meiyanto E, Agustina D, Suparjan AM, Da IM. PVG-O induces apoptosis on T47D breast cancer cells line through caspase-3 activation. *Jurnal Kedokteran Yarsi* 2007;15:75–9.
31. Leiro J, Garcia D, Arranz JA, Delgado R, Sanmartin ML, Orallo F. An Anacardiaceae preparation reduces the expression of inflammation related genes in murine macrophages. *Int Immunopharmacol* 2004;4:991–1003.
32. Rahman I, MacNee W. Regulation of redox glutathione levels and gene transcription in lung inflammation: therapeutic approaches. *Free Radic Biol Med* 2000;28:1405–20.
33. Ohshima H, Yoshie Y, Sebastien A, Gilibert I. Antioxidant and pro-oxidant actions of flavonoids: effects on DNA damage induced by nitric oxide, peroxynitrite and nitroxyl anion. *Free Radic Biol Med* 1998;25:1057–65.
34. Simon JH, Paulino AC, Smith RB, Buatti JM. Prognostic factors in head and neck rhabdomyosarcoma. *Head Neck* 2002;24:468–73.
35. Pardo-Andreu GL, Delgado R, Velho JA, Curti C, Vercesi AE. Mangiferin, a natural occurring glucosylxanthone, increases susceptibility of rat liver mitochondria to calcium induced permeability transition. *Arch Biochem Biophys* 2005;439:184–93.
36. Ravalli S, Albala A, Ming M, Szabolcs M, Barbone A, Michler RE, et al. Inducible nitric oxide synthase expression in smooth muscle cells and macrophages of human transplant coronary artery disease. *Circulation* 1998;97:2338–45.
37. Santos-Silva MC, Freitas MS, Assrey J. Involvement of NF- $\kappa$ B and glutathione in cytotoxic effects of nitric oxide and taxol on human leukemia cells. *Leuk Res* 2006;30:145–52.
38. Rosenberg MD, Colvin OM, Griffith OW, Bigner SH, Elion GB, Horton JK, et al. Establishment of a melphalan-resistant rhabdomyosarcoma xenograft with cross-resistance to vincristine and enhanced sensitivity following buthionine sulfoximine-mediated glutathione depletion. *Cancer Res* 1989;49:6917–22.
39. Porter NA. Mechanisms for the autoxidation of polyunsaturated lipids. *Acc Chem Res* 1986;19:262–8.
40. Taysi S, Polat F, Gul M, Sari RA, Bakan E. Lipid peroxidation, some extracellular antioxidants, and antioxidant enzymes in serum of patients with rheumatoid arthritis. *Rheumatol Int* 2002;21:200–4.
41. Awad HM, Boersma MG, Vervoort J, Rietjens IM. Peroxidase-catalyzed formation of quercetin quinone methide–glutathione adducts. *Arch Biochem Biophys* 2000;378:224–33.
42. Walle T, Vincent TS, Walle UK. Evidence of covalent binding of the dietary flavonoid quercetin to DNA and protein in human intestinal and hepatic cells. *Biochem Pharmacol* 2003;65:1603–10.
43. Ravid A, Rocker D, Machlenkin A, Rotem C, Hochman A, Kessler-Ickson G, et al. Dihydroxyvitamin D<sub>3</sub> enhances the susceptibility of breast cancer cells to doxorubicin-induced oxidative damage. *Cancer Res* 1999;59:862–7.
44. Filippin L, Magalhaes PJ, Di Benedetto G, Colella M, Pozzan T. Stable interactions between mitochondria and endoplasmic reticulum allow rapid accumulation of calcium in a subpopulation of mitochondria. *J Biol Chem* 2003;278:39224–34.
45. Campanella M, Szabadkai G, Rizzuto R. Modulation of intracellular Ca<sup>2+</sup> signalling in HeLa cells by the apoptotic cell death enhancer PK11195. *Biochem Pharmacol* 2008;76:1628–36.
46. Crompton M. The mitochondrial permeability transition pore and its role in cell death. *Biochem J* 1999;341:233–49.
47. Huayi H, Chaozan N, Lingxiao G. The proliferation inhibition effect and apoptosis induction of mangiferin on BEL-7404 human hepatocellular carcinoma cell. *Chin J Digest* 2002;6:341–3.
48. Xu L, Wang F, Xu X, Mo W, Huang Y, Wang X, et al. Inhibition of hepatocellular carcinoma HepG2 cell line through down-regulation of expression of microRNA-151 by resveratrol. *J Shanghai Jiaotong Univ (Med Sci)* 2010;30:774.
49. Shoji K, Tsubaki M, Yamazoe Y, Satou T, Itoh T, Kidera Y, et al. Mangiferin induces apoptosis by suppressing Bcl-xL and XIAP expressions and nuclear entry of NF- $\kappa$ B in HL-60 cells. *Arch Pharm Res* 2011;34:469–75.